Cell. Mol. Life Sci. 65 (2008) 840 – 850
1420-682X/08/050840-11
DOI 10.1007/s00018-008-7494-7

Cellular and Molecular Life Sciences

Research Article

Evidence for the intracellular accumulation of anandamide in adiposomes

S. Oddi[a, b, †], F. Fezza[b, c, †], N. Pasquariello[a], C. De Simone[b, c], C. Rapino[a], E. Dainese[a], A. Finazzi-Agrò[c] and M. Maccarrone[a, b, *]

[a] Department of Biomedical Sciences, University of Teramo, Piazza A. Moro 45, 64100 Teramo (Italy), Fax: +39-0861-266877, e-mail: mmaccarrone@unite.it
[b] European Center for Brain Research (CERC)/IRCCS S. Lucia Foundation, 00143 Rome (Italy)
[c] Department of Experimental Medicine and Biochemical Sciences, University of Rome Tor Vergata, 00133 Rome (Italy)

Received 24 October 2007; received after revision 8 January 2008; accepted 9 January 2008
Online First 24 January 2008

Abstract. Anandamide is a lipid messenger that carries out a wide variety of biological functions. It has been suggested that anandamide accumulation involves binding to a saturable cellular component. To identify the structure(s) involved in this process, we analyzed the intracellular distribution of both biotinylated and radiolabeled anandamide, providing direct evidence that lipid droplets, also known as adiposomes, constitute a dynamic reservoir for the sequestration of anandamide. In addition, confocal microscopy and biochemical studies revealed that the anandamide-hydrolase is also spatially associated with lipid droplets, and that cells with a larger adiposome compartment have an enhanced catabolism of anandamide. Overall, these findings suggest that adiposomes may have a critical role in accumulating anandamide, possibly by connecting plasma membrane to internal organelles along the metabolic route of this endocannabinoid.

Keywords. Adiposomes, biotin, endocannabinoids, lipid accumulation, lipid storage.

Introduction

In the last decade, a large body of evidence has been accumulated to support the role of the endogenous cannabinoid anandamide (*N*-arachidonoylethanolamine, AEA) as a lipid messenger, which elicits a variety of biological actions both in the central nervous system and in the periphery [1–3]. In addition, a robust therapeutic potential for the modulation of AEA signaling has been shown in an ever-growing number of pathological conditions, including chronic pain, arthritis, anxiety, glaucoma, eating disorders and infertility [1, 4]. The molecular targets through which AEA triggers its signaling pathways are type-1 (CB1R) and type-2 (CB2R) cannabinoid receptors [5], and the vanilloid receptor (TRPV1) [6]. On the other hand, the biological activity of AEA depends on its endogenous tone, which is controlled by the enzymes responsible for the synthesis and the degradation of AEA, the most identifiable of which are, *N*-acylphosphatidylethanolamines (NAPE)-hydrolyzing phospholipase D (NAPE-PLD) [7] and fatty acid amide hydrolase (FAAH) [8], respectively.

A hot topic in endocannabinoid signaling is the mechanism responsible for the transport of AEA

† These authors contributed equally to the study.
* Corresponding author.

across the plasma membrane [9], while the fate of AEA itself, once accumulated intracellularly, also remains to be clarified [10]. The transmembrane movement of AEA has been studied in several laboratories, with a primary focus on the intracellular accumulation of AEA following its exogenous administration. Although there are some areas of consensus among different groups about AEA accumulation, several aspects are still under debate. In particular, there is no consensus on the importance of FAAH-mediated hydrolysis of AEA in maintaining the driving force for AEA accumulation [11–13]. Moreover, since the active transport of AEA has been ruled out, it remains to be explained how non-metabolized AEA can be accumulated within the cell up to levels well above the concentration gradient [10, 14]. In this context, it has been suggested that an organized system of sequestration has to be present for the rapid and efficient accumulation of AEA, and for its delivery to FAAH [10, 15]. On the basis of this model, AEA movement across the plasma membrane could involve the interaction with a saturable cellular component, but experimental evidence for such an interaction has never been reported. Interestingly, recent data suggests that lipid rafts/caveolae are involved in the transmembrane transport of AEA, as well as in its recycling after catabolism [16]. To date, the identity of the component(s) necessary for the storage and/or transport of AEA within the cell has not been elucidated, primarily because of methodological constraints.

Here, we used a biotinylated derivative of AEA (biotin-AEA, b-AEA) [17], to visualize the intracellular accumulation of this endocannabinoid through immunomicroscopy. By means of biochemical analyses, we showed that biotinylation of the polar head of AEA, while preventing its interaction with FAAH, CB1R, and TRPV1, did not significantly alter the lipophilicity of this endocannabinoid, neither did it change its ability to be taken up by the cells. Although b-AEA was not hydrolyzed by FAAH, we found that it was quickly accumulated by the cells yielding a spotted pattern throughout the cytosol with a particular intensity around the nucleus. A considerable part of the vesicular-like staining of b-AEA was associated with cytosolic compartments called lipid droplets (LDs, lipid bodies or adiposomes) [18] in human keratinocytes as well as in other cell lines. This association was corroborated by the finding that cells with enlarged LDs display an increased capacity to accumulate and catabolyze AEA. Finally, by means of subfractionation and immunofluorescence studies, we showed that tritiated AEA was rapidly and dynamically accumulated within adiposomes, and that FAAH may have access to AEA in LDs through a morpho-functional connection with these organelles.

Materials and methods

Chemicals. [Arachidonyl-5,6,8,9,11,12,14,15–^{3}H]AEA (205 Ci/mmol), [^{3}H]oleic acid (60 Ci/mmol), and [^{3}H]arachidonic acid (AA) (99 Ci/mmol) were from Perkin-Elmer Life Sciences, Inc. (Boston, MA). [Ethanolamine-1–^{3}H]AEA (60 Ci/mmol) was purchased from ARC (St. Louis, MO). b-AEA and [^{3}H]b-AEA were synthesized as described [17]. URB597 was from Cayman Chemical (Ann Arbor, MI). SR141716 was a kind gift from Sanofi-Aventis Recherche (Montpellier, France). OMDM-1 was purchased from Alexis (San Diego, CA). Nonyl acridine orange, mouse anti-biotin antibody, goat Alexa Fluor-conjugates secondary antibodies, Image-iT^{TM} FX signal enhancer and Prolong antifade kit were purchased from Molecular Probes (Eugene, OR). All other chemicals were from Sigma Chemical Co. (St. Louis, MO).

Cell cultures and treatments. HaCaT and SH-SY5Y were maintained in DMEM or RPMI supplemented with 10% fetal bovine serum and cultured as described [19, 20]. To increase triacylglycerol synthesis and storage in the cells, 100 μM oleic acid complexed to albumin was added to the medium, and cells were incubated overnight at 37°C in a 5% CO_2 humidified atmosphere [21].

Biochemical analyses. FAAH activity was assayed in HaCaT cell or liver extracts, by measuring the release of [^{3}H]AA from [arachidonyl-5,6,8,9,11,12,14,15–^{3}H]AEA ([^{3}H]AEA) or [arachidonyl-5,6,8,9,11,12,14,15–^{3}H]b-AEA ([^{3}H]b-AEA) through reverse phase (RP)-HPLC [22]. In some experiments, FAAH activity was also measured in intact HaCaT cells, by measuring the release of ethanolamine-1–^{3}H from [ethanolamine-1–^{3}H]AEA under the same conditions used for the assay of AEA transport. Briefly, after [ethanolamine-1–^{3}H]AEA incubation, the reaction was stopped by adding 2 mL chloroform:methanol (2:1, v/v), and radioactivity of the water phase was measured in a beta counter. The activity of AEA transport was studied in intact HaCaT cells as described [23]. Cells were incubated for 10 min at 37°C with [^{3}H]AEA or [^{3}H]b-AEA, and were washed three times with phosphate-buffered saline (PBS) containing 1% bovine serum albumin (BSA); they were then resuspended in 0.5 mL 0.5 M NaOH, and radioactivity was measured in a scintillation counter. To further discern nonspecific transport of [^{3}H]AEA

or [^{3}H]b-AEA across cell membranes, control experiments were carried out at 4°C. The effect of 10 μM OMDM-1 on the uptake of [^{3}H]AEA or [^{3}H]b-AEA was determined by adding it directly to the incubation medium. For cannabinoid receptor studies, membrane fractions were prepared from HaCaT cells as reported [23]. These fractions were used to perform direct binding experiments of [^{3}H]AEA or [^{3}H]b-AEA by rapid filtration assays. In all experiments, unspecific binding was determined in the presence of cold agonist. Also the effect of SR141716 (1 μM) on CB1R binding was tested by adding it directly to the incubation buffer [23]. Low-energy conformations of AEA and b-AEA were calculated using the HyperChem™ 6.03 Molecular Modeling System (Hypercube, Inc., Gainesville, FL). Structural models were obtained using a molecular mechanics geometry optimization with the AMBER94 force field, followed by single point calculations. Furthermore, the following quantitative structure-activity relationship (QSAR) descriptors were calculated from the structural models of AEA and b-AEA: (i) the lipophilicity (logP value, *i.e.*, the logarithm of the *n*-octanol/water partition coefficient), using the atom fragment method developed by Ghose and Crippen [24]; and (ii) the distribution of electrostatic potentials, calculated as the potential energy of unit positive charge interacting with the analyzed molecular system [25].

Fluorescence microscopy studies. HaCaT cells were plated on collagen-coated glass coverslips. At 24 h after plating, cultures were treated either with 5 μM biotin-tag, as negative control, or with 5 μM b-AEA for 10 min at 37°C in a 5% CO_2 humidified atmosphere. After each treatment, cells were extensively washed, fixed with 4% paraformaldehyde for 30 min at room temperature, and then permeabilized with 0.1% Triton X-100 in PBS for 2 min at 4°C. After a blocking step in Image-iT™ FX signal enhancer for 30 min, cells were incubated for 1 h with anti-biotin primary antibody, diluted 1:100 in Image-iT™ FX signal enhancer. Staining of FAAH was performed using anti-FAAH diluted 1:200. Secondary antibodies conjugated to Alexa Fluor 488 or Alexa Fluor 568 were diluted 1:200 in blocking solution, and were incubated with the specimens for 30 min at room temperature. After washing, the coverslips were mounted using the antifade prolong Gold reagent, and were visualized by Nikon Eclipse E800 fluorescence microscopy (Nikon Instruments, Tokyo, Japan). To visualize lipid droplets, 100 ng/mL Nile Red dye was added to the medium 15 min before fixation, and then during incubation with antibodies.

Subcellular fractionation of [^{3}H]AEA-treated cells. HaCaT cells were grown overnight in the presence of 100 μM oleic acid; they were then collected with trypsin, washed twice with Ca^{2+}/Mg^{2+}–free HBSS, and resuspended in DMEM supplemented with 0.5% fetal bovine serum. Subsequently, cells were preincubated for 10 min with 100 nM URB597 to inhibit FAAH activity. [^{3}H]AEA or [^{3}H]oleic acid (2 μCi/10^8 cells), or nonyl acridine orange (10 μM) was added to the cells and maintained for 15 min under continuous agitation. Lipid bodies were isolated essentially as described [21]. Briefly, cells were washed twice with Ca^{2+}/Mg^{2+}–free HBSS and resuspended in 3 mL of disruption buffer (25 mM Tris-HCl, 100 mM potassium chloride, 1 mM EDTA, and 5 mM EGTA, pH 7.4, supplemented with 10 μg/mL leupeptin, 0.7 μg/mL pepstatin A, and 0.1 mM phenylmethylsulfonyl fluoride). Cells were disrupted by dounce homogenizer and mixed with an equal volume of disruption buffer containing 1.08 M sucrose. After centrifugation at 1500 *g* for 10 min to spin down nuclei, the supernatant was transferred to a 12-mL ultracentrifugation tube, and was overlaid sequentially with 2.0 mL each of 0.27 M sucrose buffer, 0.13 M sucrose buffer, and Top solution (25 mM Tris-HCl, 1 mM EDTA, and 1 mM EGTA, pH 7.4), followed by centrifugation at 150 500 *g* for 2 h. Eight fractions of 1.5 mL were collected from top to bottom: the buoyant lipid bodies (1 and 2), the mid-zone between lipid bodies and cytosol (3 and 4), and the cytosol (5–8). The microsomal pellet and nuclei (pt) were washed and resuspended in 1.5 mL Top solution by sonication. Aliquots of all nine fractions were used for the analysis of protein content, radioactivity or fluorescence (λ_{ex} = 450 nm; λ_{em} = 640 nm). To determine tritium content, 100 μL of each fraction was added to individual scintillation vials containing 3.5 mL UltimaGold XR (Perkin-Elmer; Boston, MA), and tritium was quantified in a Beckman LS 6000IC scintillation counter (Fullerton, CA).

To analyze the amount of intact [^{3}H]AEA, the fractions were extracted with a mixture of chloroform:methanol (2:1, v/v), the organic phase was dried and the pellet was subjected to RP-HPLC analysis on a Nelson 1022 Plus Chromatograph (Perkin Elmer). The separation of [^{3}H]AEA and [^{3}H]AA was carried out on a C18 (5 μm×3.0 mm×150×mm) column (Waters; Milford, MA), with a mobile phase of methanol:water:acetic acid (85:15:0.1, v/v/v) at a flow rate of 0.8 mL/min [22]. The identity of radiolabeled [^{3}H]AEA and [^{3}H]AA was confirmed by monitoring through UV detection the separation of authentic cold standards, and radioactivity was quantified by a TRI-CARB 2100TR counter (Perkin-Elmer).

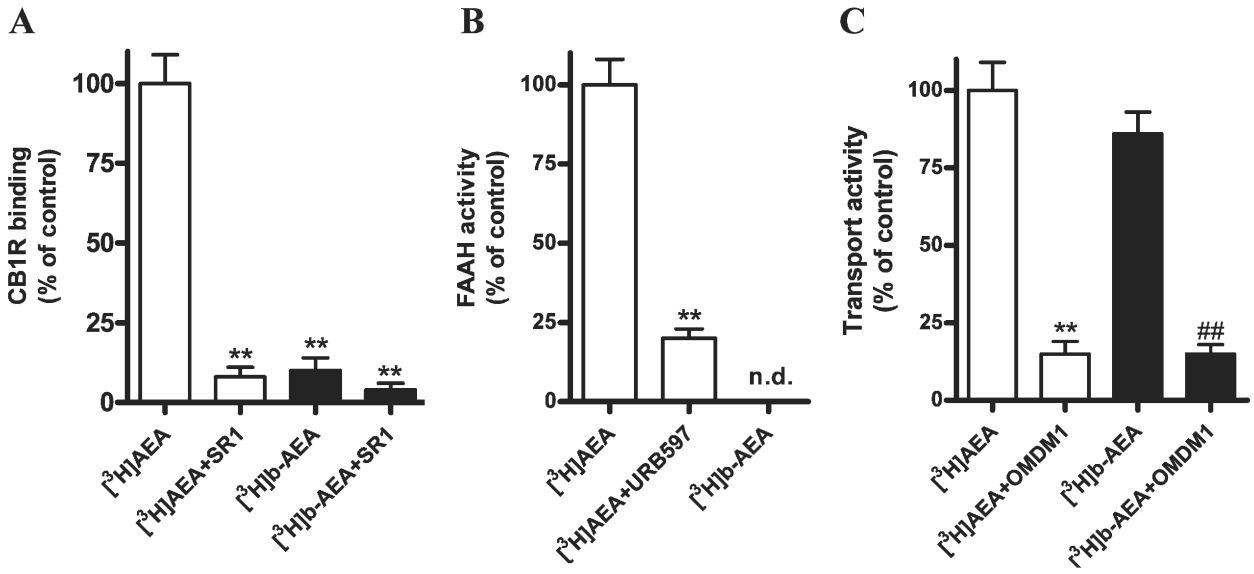

Figure 1. Comparison of the biochemical properties of *N*-arachidonoylethanolamine (AEA) and biotin-AEA (b-AEA) in HaCaT cells. (*A*) Binding of 600 nM [^{3}H]AEA (100 % control= 710±70 fmol/mg protein) and 600 nM [^{3}H]b-AEA, in the absence or in the presence of 1 μM SR141716 (SR1). (*B*) Hydrolysis of 15 μM [^{3}H]AEA (100 % control= 200±20 pmol/min per mg protein), in the absence or in the presence of 100 nM URB597, and 15 μM [^{3}H]b-AEA by fatty acid amide hydrolase (FAAH); n.d. = not detectable. (*C*) Uptake of 400 nM [^{3}H]AEA (100 % control= 83±7 pmol/min per mg protein) and 400 nM [^{3}H]b-AEA, in the absence or in the presence of 10 μM OMDM-1. In all panels, ** $p<0.001$ *versus* control, $^{\#\#}$ $p<0.001$ *versus* [^{3}H]b-AEA, and vertical bars represent ± SD values ($n=6$).

Western blot analysis. Western blotting was performed according to standard procedures [23]. The following antibodies were used to immunodetect specific markers of different subcellular compartments: anti-actin (cytosol), anti-ER (endoplasmic reticulum), anti-caveolin-1 (caveolae), anti-Na^+/K^+-ATPase (plasma membrane), and anti-adipophilin (lipid droplets). All the antibodies were purchased from Santa Cruz Biotechnology, Inc. (Santa Cruz, CA).

Statistical analysis. Data reported in this paper are the means ± SD of at least three independent experiments, each performed in duplicate. Statistical analysis was performed by the nonparametric Mann-Whitney U test, elaborating experimental data by means of the InStat 3 program (GraphPAD Software for Science, San Diego, CA).

Results

Biochemical characterization of b-AEA. In preliminary experiments, we checked the interaction of b-AEA with the elements of the endocannabinoid system [17]. Human keratinocyte HaCaT cells were chosen because they have a full and functional endocannabinoid system [23], and are suitable for immunomicroscopy studies [20]. The main results of these biochemical assays are summarized in Figure 1, and show CB1R binding, FAAH activity and transmembrane transport of AEA *versus* b-AEA under saturating concentrations.

We found that binding of b-AEA was less than 10 % of that of AEA (Fig. 1A), and that b-AEA was not at all hydrolyzed by FAAH (Fig. 1B). In fact, we found only intact [^{3}H]b-AEA when we analyzed by RP-HPLC the organic extract of the enzymatic reaction, demonstrating that b-AEA is metabolically stable. On the other hand, HaCaT cells were able to accumulate [^{3}H]b-AEA to almost the same extent as [^{3}H]AEA (Fig. 1C), and the uptake of both compounds was strongly reduced by 10 μM OMDM-1 (Fig. 1C), a selective inhibitor of AEA transport [26]. HaCaT cells do not express TRPV1 receptors [23]; however, binding of 500 pM [^{3}H]resinferatoxin (a specific agonist of TRPV1) to C6 glioma cell membranes was not displaced by b-AEA at concentrations higher than 10 μM [17]. Taken together, these data suggest that b-AEA, unlike AEA, is not hydrolyzed by FAAH, and does not activate CB1R or TRPV1 receptors, nor subsequent signaling pathways; yet, b-AEA is transported in the same manner as AEA. Furthermore, these findings are consistent with previous studies indicating that the kinetics of AEA uptake is sensitive to modification of the arachidonate moiety, whereas changes in the ethanolamide region are ineffective [27, 28].

To gain further insights into the properties of these compounds, we calculated some relevant QSAR

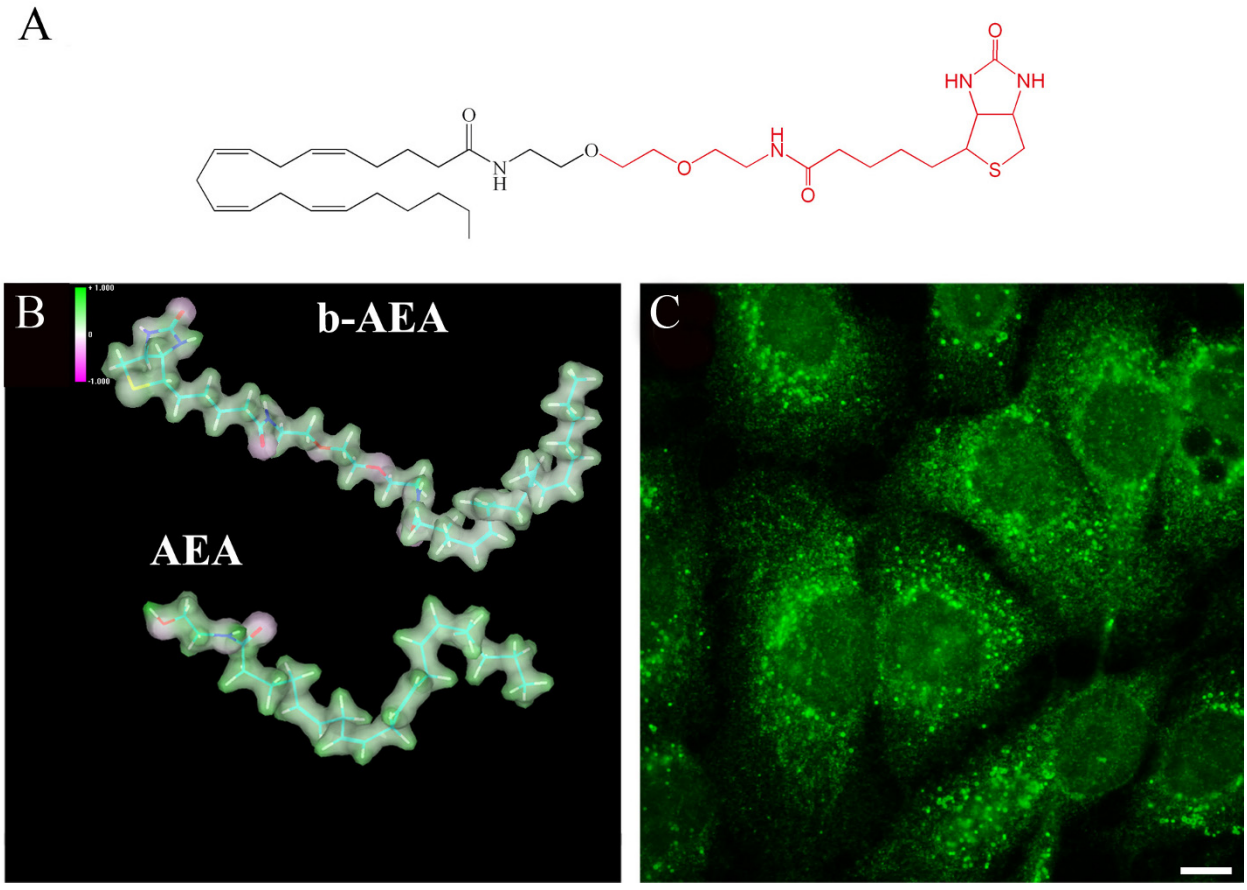

Figure 2. Molecular structure, electrostatic potential and immunofluorescence detection of b-AEA in HaCaT cells. (*A*) Chemical structure of b-AEA: the anandamide and biotin moieties are colored in black and in red, respectively. (*B*) Low-energy conformations of AEA and b-AEA, showing the electrostatic potential (violet –1; green + 1) on the molecular surface. (*C*) Immunofluorescence detection of b-AEA in HaCaT cells. b-AEA was quickly accumulated by the cells decorating several structures inside the cytoplasm. The image is representative of three independent experiments, and in each case five fields were examined. Bar 10 μm.

parameters. This approach revealed that the addition of the biotin-tag to AEA did not change the general lipophilic character of the molecule, expressed as logP (5.1 for AEA and 4.7 for b-AEA). In fact, logP values higher than ~4.5 are indicative of very lipophilic molecules [24], and for both AEA and b-AEA they suggest that less than 1 molecule out of 50 000 is dissolved in water. This is in accordance with low-energy conformations of AEA and b-AEA, which display similar distributions of electrostatic potentials on the acyl chain moiety (Fig. 2B). However, it should be noted that the *in vivo* significance of these QSAR descriptors remains to be ascertained.

Visualization of the intracellular distribution of b-AEA in HaCaT cells. The immunostaining performed with an anti-biotin monoclonal antibody showed that HaCaT cells quickly (within 5 min) accumulated b-AEA, yielding a spotted pattern throughout the cytosol and in close proximity to the nucleus (Fig. 2C). Since b-AEA is not hydrolyzed by FAAH (Fig. 1B), this finding corroborates the notion that FAAH activity is not strictly required for the transmembrane movement or cellular accumulation of AEA, as clearly demonstrated in *faah*-null cells [13, 29], as well as in cells with very low FAAH activity [11] or in reconstituted plasma membrane vesicles [20]. As the biotin-tag *per se* was not taken up by the cells under the same experimental conditions (data not shown), the particular distribution of b-AEA could not be attributed to the biotin moiety of the probe. In line with this, we found that biotinyl-arachidic acid, a saturated analogue of b-AEA, was not transported inside the cells (data not shown), further supporting that it is the arachidonic moiety and not the biotin-tag of b-AEA that is the crucial portion for a correct transport of the molecule across the cell membranes. Furthermore, immunofluorescence microscopy inspections showed a consistency of the spotted pattern of the cells with vesicles that resembled ring-like structures reminiscent of lipid droplets (LDs). These are cytosolic organelles ubiquitously present in eu-

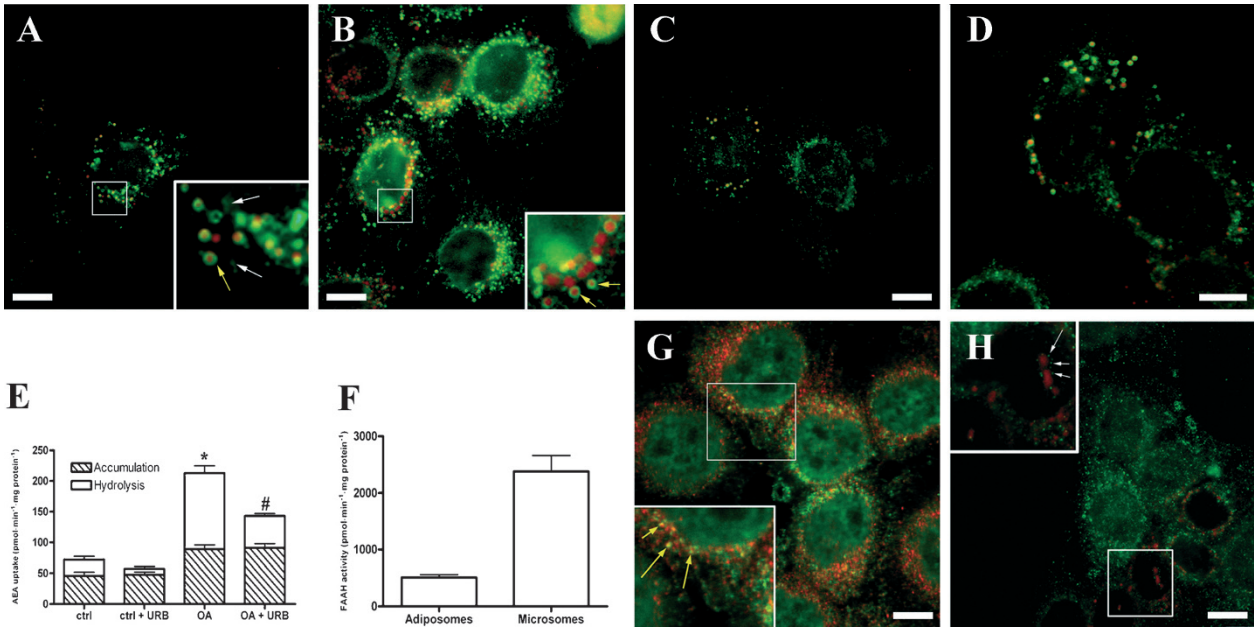

Figure 3. Immunocytochemical localization of b-AEA and FAAH to cytoplasmic lipid droplets (LDs) in human HaCaT cells. (*A*) LDs in HaCaT cells were stained with Nile Red (red). Cells grown in normal (*i.e.*, low-lipid containing) medium showed colocalization of b-AEA (green) with the rim of the round-shaped lipid bodies (magnified box, yellow arrows). A residual staining seems to be distinct from LDs having a more undefined cytosolic distribution (magnified box; white arrows). (*B*) Cells treated overnight with 100 μM oleic acid/BSA displayed a significant increase in b-AEA staining, which paralleled the increase of LDs size. (*C*) Serum-starved cells (*i.e.*, low oleic acid condition) showed a significant reduction of the LDs compartment and a parallel reduction in the accumulation of b-AEA. (*D*) Immunodetection of b-AEA in SH-SY5Y cells. Images are representative of at least three independent experiments, and five fields were examined for each treatment. (*E*) Effect of oleic acid treatment (OA) *versus* control (ctrl) on [^{3}H]AEA uptake by HaCaT cells, grown in the absence or in the presence of 100 nM URB597. In (*E*), * $p<0.05$ *versus* ctrl, and $^{\#}$ $p<0.05$ *versus* ctrl + URB597 ($n=4$). (*F*) Analysis of the FAAH-specific activity in the adiposome fraction and microsome fraction obtained by mouse liver subfractionation. (*G*) Co-staining of HaCaT cells with anti-FAAH (green) and anti-biotin (red) antibodies. The superimposition of the two stainings revealed that FAAH and b-AEA colocalize only in dot structures near to the perinuclear region (yellow arrows in the inset). (*H*) Co-staining of HaCaT cells with anti-FAAH antibodies (green) and Nile red staining for adiposomes (red). The superimposition of the two stainings revealed that several FAAH-positive dots are associated to the periphery of the LDs (white arrows in the inset). Bars, 10 μm.

karyotic cells, where they act as a storage compartment for neutral lipids [18]. LDs, also called lipid bodies or adiposomes, contain a neutral lipid core of triacylglycerols and sterol esters, and are selectively stained by the phenoxazine dye Nile Red [30]. Their lipid core is surrounded by a phospholipid monolayer that interacts with LDs-associated proteins. We found that b-AEA staining was diffused throughout the cytoplasm (Fig. 3A), and that it formed rings surrounding the Nile-Red positive central core of adiposomes (Fig. 3A, inset). These observations suggest that intracellular b-AEA reaches the adiposomes and is stored on their surface. In addition to HaCaT cells (Fig. 3A, inset), b-AEA colocalized with adiposomes also in human neuronal SH-SY5Y cells (Fig. 3D), and immune U937 cells (data not shown).

To further investigate the functional link between b-AEA and LDs, the dimension of the adiposome compartment was reduced by cell starvation. In fact, the amount of oleic acid present in the medium, and hence the adiposome size, is reduced as a consequence of starvation [31]. In serum-starved cells we observed a marked reduction of b-AEA accumulation, which paralleled the reduction of number and size of LDs (Fig. 3C). On the other hand, feeding HaCaT cells with an additional supply of oleic acid considerably increased the uptake of b-AEA, again paralleling the increase in size and number of LDs (Fig. 3B).

The dependence of AEA accumulation on the dimension of LDs was confirmed also by examining the uptake of 400 nM [^{3}H]AEA by HaCaT cells grown with an excess of oleic acid. The net uptake of [^{3}H]AEA in oleic acid-treated cells was approximately threefold higher than that of controls (Fig. 3E). Since the internalization of AEA is thought to be the result of two different processes, *i.e.*, accumulation through saturable intracellular components, and FAAH-mediated hydrolysis, we sought to estimate the contribution of AEA hydrolysis by inactivating FAAH with 100 nM URB597 [32]. The enzymatic activity of FAAH in living cells was measured using 400 nM [ethanolamine-1–^{3}H]AEA as substrate under the same conditions used for the assay of AEA

transport. The addition of URB597 did not abolish completely FAAH activity, which remained ~40 % and ~35 % of that of oleate-treated and untreated cells (Fig. 3E, white bars); yet, the partial inhibition of AEA degradation reduced the net uptake of [^{3}H]AEA by ~30 % of the controls, both in oleate-treated and untreated cells (Fig. 3E). This observation suggests that FAAH activity, although not a requisite for AEA accumulation, does contribute to this process by maintaining a concentration gradient across the plasma membrane. The contribution of AEA hydrolysis was estimated by the difference between the AEA uptake in the absence and in the presence of URB597, corrected for residual FAAH activity. On this basis, we found that AEA catabolism by FAAH was approximately fivefold faster in oleate-treated cells than in controls, and that the intracellular accumulation of AEA was approximately twofold higher in LDs-enriched cells than in controls (Fig. 3E, hatched bars). These data further indicate that adiposomes are directly involved in the intracellular accumulation of AEA. Since FAAH activity in oleate-treated cell homogenates was comparable to that of controls (122±17 *versus* 116±10 pmol/min per mg protein), we also speculated that the higher catabolism of AEA observed in treated cells might be due to a faster shuttling of AEA from plasma membrane to intracellular degradation sites, made possible by adiposomes. In line with this hypothesis, we found by immunofluorescence experiments that b-AEA internalized in HaCaT cells reached the endoplasmic reticulum near the nucleus, where it partially co-localized with FAAH staining (Fig. 3G, yellow arrows in inset). Furthermore, the existence of a morpho-functional overlap between LDs and FAAH was ascertained by co-fractionation studies, which revealed a small but significant amount of FAAH activity associated with adiposome-rich fraction derived from mouse liver (Fig. 3F). Additional co-localization studies revealed that FAAH-positive dots (Fig. 3H, green) were partly associated with the periphery of LDs in HaCaT cells (Fig. 3H, white arrows in inset). Incidentally, these findings confirm the results of a recent proteomic study, which demonstrated the presence of FAAH in purified LDs from *Drosophila* embryos [33].

Storage of AEA in adiposome-rich fractions of HaCaT cells. The relationship between AEA and LDs was also investigated by analyzing the intracellular distribution of [^{3}H]AEA after its uptake. We performed subcellular fractionation of HaCaT cells grown in the presence of an excess of oleic acid, and incubated for 15 min with [^{3}H]AEA. To prevent the degradation of AEA, FAAH was inactivated by preincubating the cells for 10 min with 100 nM URB597. LDs were isolated by flotation [21] and characterized by fluorescence staining and Western blotting [21]. The two top fractions of the gradient (1 and 2), containing only 1 % of the total proteins, were positive for adipophilin, an LD-specific protein, and were devoid of markers of caveolae (caveolin-1), endoplasmic reticulum (ER), cytosol (actin) and plasma membranes (Na^+/K^+-ATPase) (Fig. 4A). Fluorescence microscopy of Nile Red-stained fractions showed bright, spotted and spherical lipid bodies in all fractions of the gradient, the greatest amount being present in fraction 1 and the smallest amount in fractions 4–8 (Fig. 4B).

The distribution of [^{3}H]AEA in these fractions was quantified by radioactivity, normalized to the protein content. We found that the two fractions containing LDs (1 and 2) were also the richest in [^{3}H]AEA (Fig. 4C), further suggesting that adiposomes were important sites for the accumulation of AEA. The [^{3}H]AEA subcellular profile was mirrored by that obtained with [^{3}H]oleic acid, a lipid molecule that is known to specifically accumulate in LDs (Fig. 4D). In addition, to exclude nonspecific associations with LDs, we also analyzed the subcellular distribution of nonyl acridine orange. This fluorescent dye associates with cardiolipin, an anionic phospholipid abundant in mitochondria. As expected, fluorescence of nonyl acridine orange was primarily enriched in the microsomal fraction and was virtually absent from LDs (Fig. 4D). Moreover, by means of radiochromatography we found that ~85 % of radioactivity in fractions 1 and 2 was due to intact [^{3}H]AEA, giving a peak with a retention time of 2.2 min, whereas only ~15 % of radioactivity was eluted with a retention time of 3.4 min, typical of the [^{3}H]AEA hydrolysis product [^{3}H]AA (data not shown). To further support the functional interaction between AEA storage, LDs and FAAH, we demonstrated that in the absence of the FAAH inhibitor URB597 the distribution of [^{3}H]AEA markedly changed, with a reduction of radioactivity in the adiposome fraction, and a parallel increase in the microsomal fraction (Fig. 4C). Taken together, these findings demonstrate that the steady state content of AEA in LDs is dynamically regulated by FAAH activity.

Discussion

AEA signaling is critically regulated by its transport across the plasma membrane, followed by intracellular breakdown. In the last few years, the biosynthesis and degradation of AEA have been investigated in great detail, leading to the molecular cloning and

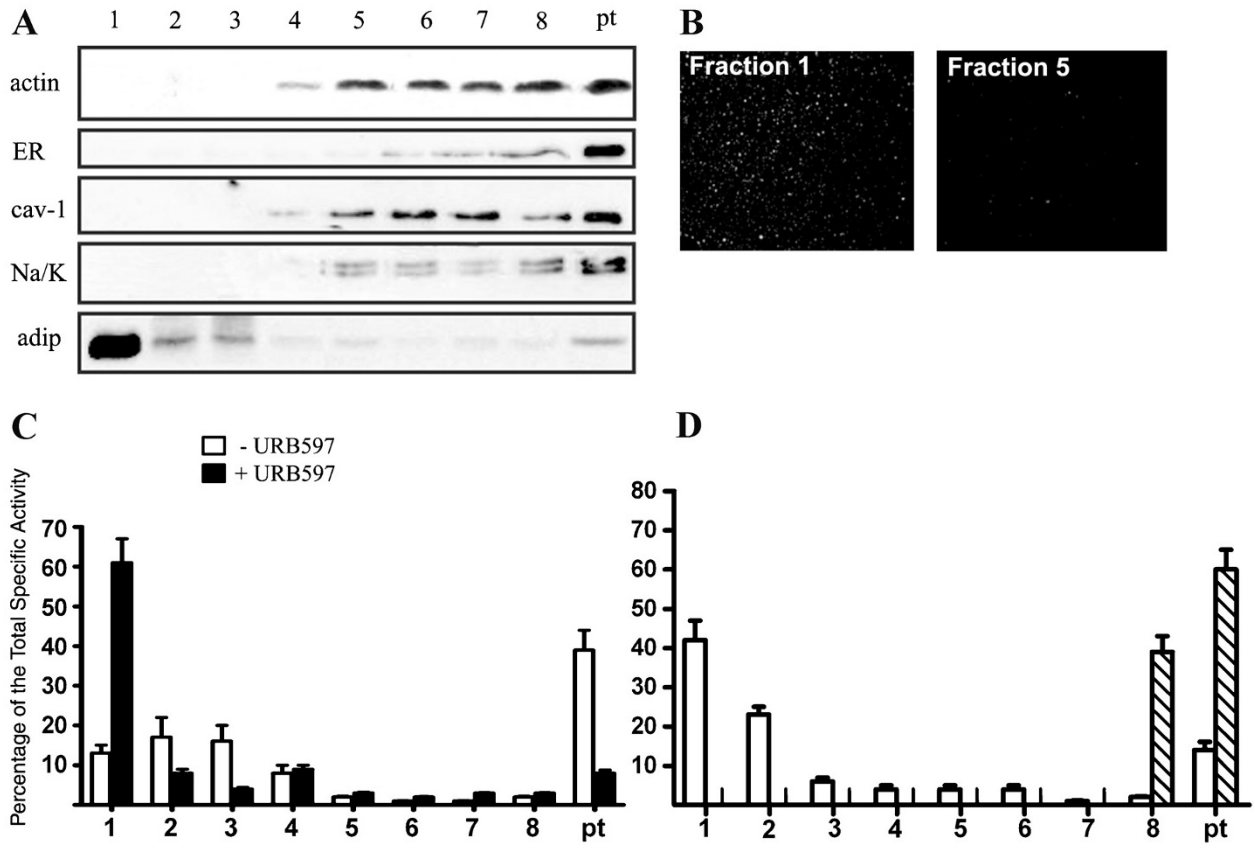

Figure 4. Subcellular distribution of internalized [^{3}H]AEA in human HaCaT cells. (*A*) The subcellular fractions obtained from HaCaT cells were analyzed by Western blotting using different markers for cytoplasm (actin), endoplasmic reticulum (ER), caveolae (caveolin-1, cav-1), plasma membrane (Na^+/K^+-ATPase, Na/K) and lipid droplets (adipophilin, adip). (*B*) Staining of fraction 1 (LDs) and fraction 5 (cytosol) with Nile Red. (*C*) Enrichment of [^{3}H]AEA in the subcellular fractions was expressed as percentage of the total specific activity. The radioactivity of accumulated [^{3}H]AEA was measured in the presence (black bars) or in the absence (white bars) of 100 nM URB597 (black bars: 100 % =430±30 dpm/μg protein; white bars: 100 % =1180±50 dpm/μg protein). (*D*) Content of ^{3}H-labeled oleate (open bars; 100 % =1400±200 dpm/μg protein), and fluorescence of nonyl acridine orange (hatched bars; 100 % = 15±20 fluorescence arbitrary units) in subcellular fractions of HaCaT cells.

characterization of the AEA hydrolase FAAH [8, 34], and of the main AEA synthetase NAPE-PLD [7]. Conversely, the molecular mechanism(s) by which AEA moves across the plasma membrane and within the cell is still a largely unclear territory [35]. The lack of information on this topic depends on the lack of suitable methods; until now methods have been essentially limited to radiometric-based techniques. In fact, although the use of radioactive AEAs – labeled on the arachidonate moiety or on the ethanolamide head – allows high sensitivity in the analysis of the kinetic features of AEA transport, it does not allow visualization of the specific pathways for internalization and intracellular accumulation. In particular, the characteristics of anandamide accumulation demonstrated in several laboratories are consistent with the hypothesis that anandamide moves across cellular membranes by binding to a saturable component. However, the identity of this component remains elusive.

Here we used a novel tool, *i.e.*, biotinylated anandamide, specifically designed to visualize AEA transport and intracellular accumulation by means of fluorescence microscopy. Previous biochemical assays clearly demonstrated that biotinylation of the polar head of AEA does not affect its ability to be taken up by the cells, while it prevents its interaction with CB1R and FAAH. More detailed kinetic or binding analyses support this concept, and they are reported elsewhere [17]. It should be recalled that the transport of AEA and its recognition by CB1R and FAAH are based on different constraints of the active/binding sites [36, 37], and that we added the biotin moiety in a position of AEA known to be tolerated by the transport mechanism only [27, 28]. In this context, the example of methanandamide seems of interest. This is a stable analogue of AEA, which is not a substrate for FAAH but is transported with a mechanism similar to that of AEA [38]. We have shown for the first time that, once taken up by the cell, AEA is rapidly targeted to lipid

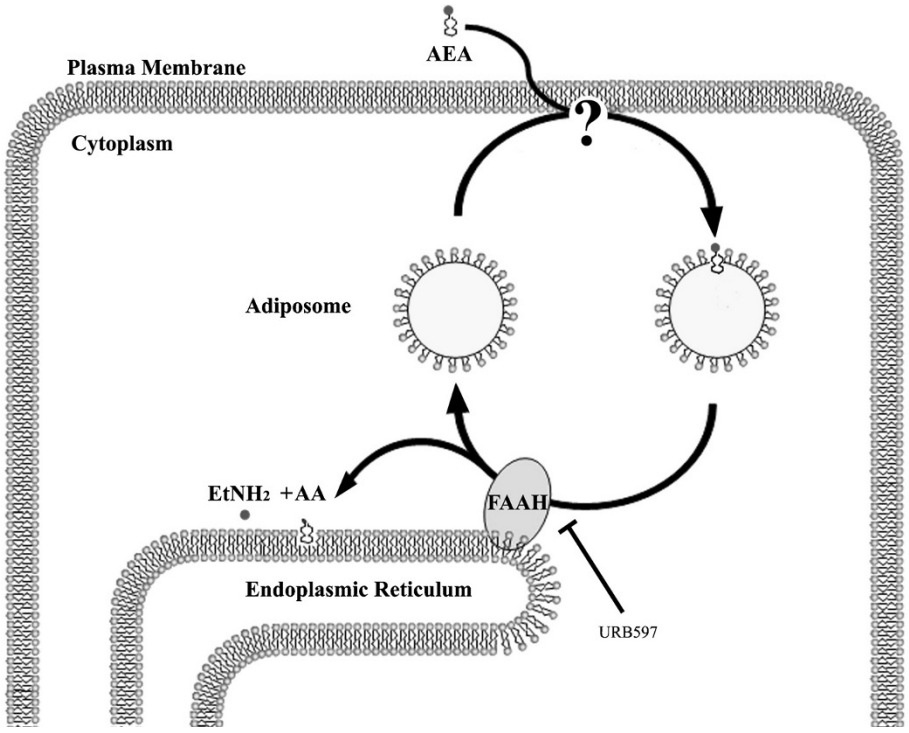

Figure 5. Hypothetical model of the role of adiposomes in transport and metabolism of anandamide. The scheme depicts the possible roles of cytosolic LDs as intracellular "sink" and "shuttle" for the accumulation and transport of AEA among specific intracellular compartments. Once internalized by an as-yet elusive mechanism, AEA is concentrated in the adiposomes, which contribute to maintaining an inward gradient that drives anandamide influx. Moreover, LDs may also enhance AEA catabolism by rapidly and efficiently shuttling LDs-bound AEA between plasma membranes and intracellular compartments, where it is hydrolyzed to arachidonic acid (AA) and ethanolamine ($EtNH_2$) by the ER- and/or LD-bound FAAH.

bodies; these ubiquitous organelles have been originally described as intracellular stores for neutral lipids and, more recently, they have been linked to transport routes pivotal for lipid trafficking, homeostasis and signaling (for a recent review see [18]). By kinetic and subfractionation studies, we also demonstrated that cells with a larger LD compartment display an increased capacity to accumulate and metabolize AEA. In line with this, it is noteworthy that the zona glomerulosa cells of the bovine adrenal cortex, one of the richest tissues in lipid-filled organelles, also exhibit the greatest capacity to accumulate AEA [11, 39]. Finally, we demonstrated an overlap between LD compartment and FAAH, which is presumably instrumental for the rapid degradation of AEA stored in these organelles.

Taken together, our findings lend biochemical support to an hypothetical model – originally proposed by Hillard and Jarrahian [10] – that predicts the existence of a cellular compartment where AEA sequestration can allow its accumulation well beyond the concentration gradient (depicted in Fig. 5). By functioning as anandamide reservoirs, adiposomes could sequestrate AEA in a form that is not in free equilibrium with the extracellular pool, thus keeping the intracellular concentration of free AEA very low. Moreover, by virtue of their high mobility within the cell [40], and of their morpho-functional connection with FAAH (this study), adiposomes can also act as shuttles for the rapid and efficient delivery of AEA from the plasma membrane to the intracellular sites, where hydrolysis takes place. Incidentally, the existence of these AEA-accumulating organelles might call for some re-conceptualization of a "dogma" of endocannabinoid biology, *i.e.*, that AEA, unlike the other neurotransmitters, is produced "on demand" and is not stored in vesicles. On the other hand, we do not quite know the biological significance of AEA storage in adiposomes, and the hypothesis that these organelles might release AEA "on demand" needs to be further addressed. We are currently performing separate immunofluorescence studies to explore this aspect and also to further characterize the intracellular trafficking of AEA.

In conclusion, the present study uncovers novel aspects of the intracellular distribution of AEA, and provides the first evidence for the involvement of adiposomes in AEA accumulation and degradation, thus adding a new player to the complex network of synthesis, uptake and hydrolysis that is responsible for the propagation of endocannabinoid signaling.

A*cknowledgements*. We wish to thank Drs. Monica Bari and Paola Spagnuolo for their valuable help in biochemical assays. This investigation was supported by Fondazione TERCAS (Research Programs 2004 and 2005 to M.M.), by Ministero dell'Università e della Ricerca (PRIN 2005 to A.F.-A. and FIRB 2006 to M.M.), and by Agenzia Spaziale Italiana (DCMC and MoMa projects 2006 to A.F.-A. and M.M.).

1 Piomelli, D. (2003) The molecular logic of endocannabinoid signalling. Nat. Rev. Neurosci. 4, 873–884.

2 Klein, T. W. (2005) Cannabinoid-based drugs as anti-inflammatory therapeutics. Nat. Rev. Immunol. 5, 400–411.
3 Bari, M., Spagnuolo, P., Fezza, F., Oddi, S., Pasquariello, N., Finazzi-Agrò, A. and Maccarrone, M. (2006) Effect of lipid rafts on Cb2 receptor signaling and 2-arachidonoyl-glycerol metabolism in human immune cells. J. Immunol. 177, 4971–4980.
4 Di Marzo, V., Bifulco, M. and De Petrocellis, L. (2004) The endocannabinoid system and its therapeutic exploitation. Nat. Rev. Drug Discov. 3, 771–784.
5 Howlett, A. C. (2002) The cannabinoid receptors. Prostaglandins Other Lipid Mediat. 68–69, 619–631.
6 van der Stelt, M. and Di Marzo, V. (2005) Anandamide as an intracellular messenger regulating ion channel activity. Prostaglandins Other Lipid Mediat. 77, 111–122.
7 Okamoto, Y., Morishita, J., Tsuboi, K., Tonai, T. and Ueda, N. (2004) Molecular characterization of a phospholipase D generating anandamide and its congeners. J. Biol. Chem. 279, 5298–5305.
8 McKinney, M. K. and Cravatt, B. F. (2005) Structure and function of fatty acid amide hydrolase. Annu. Rev. Biochem. 74, 411–432.
9 Glaser, S. T., Kaczocha, M. and Deutsch, D. G. (2005) Anandamide transport: A critical review. Life Sci. 77, 1584–1604.
10 Hillard, C. J. and Jarrahian, A. (2003) Cellular accumulation of anandamide: Consensus and controversy. Br. J. Pharmacol. 140, 802–808.
11 Hillard, C. J., Edgemond, W. S., Jarrahian, A. and Campbell, W. B. (1997) Accumulation of *N*-arachidonoylethanolamine (anandamide) into cerebellar granule cells occurs via facilitated diffusion. J. Neurochem. 69, 631–638.
12 Moore, S. A., Nomikos, G. G., Dickason-Chesterfield, A. K., Schober, D. A., Schaus, J. M., Ying, B. P., Xu, Y. C., Phebus, L., Simmons, R. M., Li, D., Iyengar, S. and Felder, C. C. (2005) Identification of a high-affinity binding site involved in the transport of endocannabinoids. Proc. Natl. Acad. Sci. USA 102, 17852–17857.
13 Glaser, S. T., Abumrad, N. A., Fatade, F., Kaczocha, M., Studholme, K. M. and Deutsch, D. G. (2003) Evidence against the presence of an anandamide transporter. Proc. Natl. Acad. Sci. USA 100, 4269–7424.
14 Deutsch, D. G., Glaser, S. T., Howell, J. M., Kunz, J. S., Puffenbarger, R. A., Hillard, C. J. and Abumrad, N. (2001) The cellular uptake of anandamide is coupled to its breakdown by fatty-acid amide hydrolase. J. Biol. Chem. 276, 6967–6973.
15 McFarland, M. J., Porter, A. C., Rakhshan, F. R., Rawat, D. S., Gibbs, R. A. and Barker, E. L. (2004) A role for caveolae/lipid rafts in the uptake and recycling of the endogenous cannabinoid anandamide. J. Biol. Chem. 279, 41991–41997.
16 McFarland, M. J., Terebova, E. A. and Barker, E. L. (2006) Detergent-resistant membrane microdomains in the disposition of the lipid signaling molecule anandamide. AAPS J. 8, E95–100.
17 Maccarrone, M., Oddi, S., Fezza, F. and Finazzi-Agrò, A. (2006) Design and synthesis of biotinylated probes for *N*-acylethanolamines. PCT/EP 2006/061988.
18 Martin, S. and Parton, R. G. (2006) Lipid droplets: A unified view of a dynamic organelle. Nat. Rev. Mol. Cell. Biol. 7, 373–378.
19 Canals, M., Angulo, E., Casado, V., Canela, E. I., Mallol, J., Vinals, F., Staines, W., Tinner, B., Hillion, J., Agnati, L., Fuxe, K., Ferre, S., Lluis, C. and Franco, R. (2005) Molecular mechanisms involved in the adenosine A and A receptor-induced neuronal differentiation in neuroblastoma cells and striatal primary cultures. J. Neurochem. 92, 337–348.
20 Oddi, S., Bari, M., Battista, N., Barsacchi, D., Cozzani, I. and Maccarrone, M. (2005) Confocal microscopy and biochemical analysis reveal spatial and functional separation between anandamide uptake and hydrolysis in human keratinocytes. Cell. Mol. Life Sci. 62, 386–395.
21 Yu, W., Cassara, J. and Weller, P. F. (2000) Phosphatidylinositide 3-kinase localizes to cytoplasmic lipid bodies in human polymorphonuclear leukocytes and other myeloid-derived cells. Blood 95, 1078–1085.
22 Maccarrone, M., Bari, M. and Finazzi-Agrò, A. (1999) A sensitive and specific radiochromatographic assay of fatty acid amide hydrolase activity. Anal. Biochem. 267, 314–318.
23 Maccarrone, M., Di Rienzo, M., Battista, N., Gasperi, V., Guerrieri, P., Rossi, A. and Finazzi-Agrò, A. (2003) The endocannabinoid system in human keratinocytes. Evidence that anandamide inhibits epidermal differentiation through CB1 receptor-dependent inhibition of protein kinase C, activation protein-1, and transglutaminase. J. Biol. Chem. 278, 33896–33903.
24 Ghose, A. K. and Crippen, G. M. (1987) Atomic physicochemical parameters for three-dimensional-structure-directed quantitative structure-activity relationships. 2. Modeling dispersive and hydrophobic interactions. J. Chem. Inf. Comput. Sci. 27, 21–35.
25 Miller, K. J. (1990) Additivity methods in molecular polarizability. J. Am. Chem. Soc. 112, 8533–8542.
26 Ortar, G., Ligresti, A., De Petrocellis, L., Morera, E. and Di Marzo, V. (2003) Novel selective and metabolically stable inhibitors of anandamide cellular uptake. Biochem. Pharmacol. 65, 1473–1481.
27 Muthian, S., Nithipatikom, K., Campbell, W. B. and Hillard, C. J. (2000) Synthesis and characterization of a fluorescent substrate for the *N*-arachidonoylethanolamine (anandamide) transmembrane carrier. J. Pharmacol. Exp. Ther. 293, 289–295.
28 Piomelli, D., Beltramo, M., Glasnapp, S., Lin, S. Y., Goutopoulos, A., Xie, X. Q. and Makriyannis, A. (1999) Structural determinants for recognition and translocation by the anandamide transporter. Proc. Natl. Acad. Sci. USA 96, 5802–5807.
29 Day, T. A., Rakhshan, F., Deutsch, D. G. and Barker, E. L. (2001) Role of fatty acid amide hydrolase in the transport of the endogenous cannabinoid anandamide. Mol. Pharmacol. 59, 1369–1375.
30 Gocze, P. M. and Freeman, D. A. (1994) Factors underlying the variability of lipid droplet fluorescence in MA-10 Leydig tumor cells. Cytometry 17, 151–158.
31 Wolins, N. E., Rubin, B. and Brasaemle, D. L. (2001) TIP47 associates with lipid droplets. J. Biol. Chem. 276, 5101–5108.
32 Kathuria, S., Gaetani, S., Fegley, D., Valino, F., Duranti, A., Tontini, A., Mor, M., Tarzia, G., La Rana, G., Calignano, A., Giustino, A., Tattoli, M., Palmery, M., Cuomo, V. and Piomelli, D. (2003) Modulation of anxiety through blockade of anandamide hydrolysis. Nat. Med. 9, 76–81.
33 Cermelli, S., Guo, Y., Gross, S. P. and Welte, M. A. (2006) The lipid-droplet proteome reveals that droplets are a protein-storage depot. Curr. Biol. 16, 1783–1795.
34 Bracey, M. H., Hanson, M. A., Masuda, K. R., Stevens, R. C. and Cravatt, B. F. (2002) Structural adaptations in a membrane enzyme that terminates endocannabinoid signaling. Science 298, 1793–1796.
35 McFarland, M. J. and Barker, E. L. (2004) Anandamide transport. Pharmacol. Ther. 104, 117–35.
36 Di Marzo, V., Ligresti, A., Morera, E., Nalli, M. and Ortar, G. (2004) The anandamide membrane transporter. Structure-activity relationships of anandamide and oleoylethanolamine analogs with phenyl rings in the polar head group region. Bioorg. Med. Chem. 12, 5161–5169.
37 Ortega-Gutierrez, S. and Lopez-Rodriguez, M. L. (2005) CB1 and CB2 cannabinoid receptor binding studies based on modeling and mutagenesis approaches. Mini Rev. Med. Chem. 5, 651–658.
38 Abadji, V., Lin, S., Taha, G., Griffin, G., Stevenson, L. A., Pertwee, R. G. and Makriyannis, A. (1994) (R)-methanandamide: A chiral novel anandamide possessing higher potency and metabolic stability. J. Med. Chem. 37, 1889–1893.

39 Hillard, C. J. and Jarrahian, A. (2000) The movement of *N*-arachidonoylethanolamine (anandamide) across cellular membranes. Chem. Phys. Lipids 108, 123–134.

40 Nan, X., Potma, E. O. and Xie, X. S. (2006) Nonperturbative chemical imaging of organelle transport in living cells with coherent anti-stokes Raman scattering microscopy. Biophys. J. 91, 728–735.